



## [Cp<sub>2</sub>TiCH<sub>2</sub>CH<sub>2</sub>(SiEt<sub>2</sub>CHMe<sub>2</sub>)]<sup>+</sup>, an Alkyl-titanocene(IV) Complex Containing an Unconventional Ti←C(β)-Si Mode of Bonding

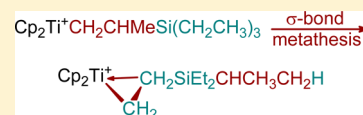
Alexandre F. Dunlop-Brière,<sup>†</sup> Michael C. Baird,<sup>\*,†</sup> and Peter H. M. Budzelaar<sup>\*,‡</sup>

<sup>†</sup>The Department of Chemistry, Queen's University, Kingston, Ontario K7L 3N6, Canada

<sup>‡</sup>Department of Chemistry, University of Manitoba, Winnipeg, Manitoba R3T 2N2, Canada

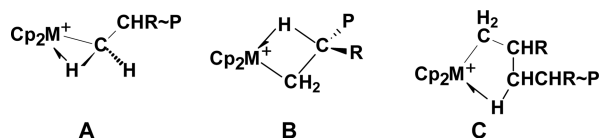
### S Supporting Information

**ABSTRACT:** The compound [Cp<sub>2</sub>Ti(Me)(CD<sub>2</sub>Cl<sub>2</sub>)] [B(C<sub>6</sub>F<sub>5</sub>)<sub>4</sub>] reacts with triethylvinylsilane (TEVS) to give the γ-agostic σ-alkyl complex [Cp<sub>2</sub>TiCH<sub>2</sub>CHMe(SiEt<sub>3</sub>)]<sup>+</sup> (IV), the product of a single 1,2-insertion of TEVS into the Ti-Me bond. On heating, complex IV undergoes a CH bond activation process to give the isomeric species [Cp<sub>2</sub>TiCH<sub>2</sub>CH<sub>2</sub>(SiEt<sub>2</sub>CHMe<sub>2</sub>)]<sup>+</sup> (V) in which a Ti←C(β) interaction (Ti←C(β)-Si) is facilitated by an unusual γ-silyl effect. The structures of IV and V and the nature of the isomerization process were explored by DFT methods which suggest that isomerization proceeds via an intramolecular 1,5-σ bond metathesis reaction which involves ε-agostic interactions.



### INTRODUCTION

Metallocene catalyzed coordination polymerization processes generally involve sequences of alkene coordination and migratory insertion steps,<sup>1</sup> the latter being facilitated by α-agostic interactions as in A (P = polymeryl) with complementary β-agostic species (B) serving as resting states during propagation; γ-agostic species C have also on occasion been invoked.<sup>2</sup> However, activation energies for the extended sequences of migratory insertion processes required for chain growth of readily polymerized alkenes such as ethylene, propylene, and 1-alkenes are generally very low, and thus lifetimes of α- and β-agostic intermediates of types A and B are too short for them to be observed as intermediates during polymerization.<sup>1–3</sup>



That said, we have shown, by using alkenes which are too sterically hindered to undergo homopolymerization via a coordination polymerization mechanism, that α- and β-agostic titanocene(IV) complexes of types A and B can be sufficiently stable for them to be detected and characterized by low temperature NMR spectroscopy.<sup>4</sup> It seems that the propagation steps in such cases are sufficiently slow that normally unstable agostic intermediates can be observed, and thus, for example, the reaction of [Cp<sub>2</sub>Ti(Me)(CD<sub>2</sub>Cl<sub>2</sub>)] [B(C<sub>6</sub>F<sub>5</sub>)<sub>4</sub>] (I) with 3,3-dimethyl-1-butene (CH<sub>2</sub>=CHCMe<sub>3</sub>) at ~200 K resulted in the formation of the α-agostic complex, [Cp<sub>2</sub>TiCH<sub>2</sub>CHMe(CMe<sub>3</sub>)]<sup>+</sup> (II), of type A.<sup>4b,d</sup> Aside from its intrinsic novelty, the α-agostic structure observed for II is also unusual because most coordinatively unsaturated metal alkyl compounds bearing β-H atoms prefer β- over α-agostic structures.<sup>5</sup>

Following our initial investigation of II,<sup>4b,d</sup> we carried out an analogous study of the reaction of I with trimethylvinylsilane CH<sub>2</sub>=CHSiMe<sub>3</sub>, TMVS),<sup>4c</sup> another alkene which seems not to be readily polymerized via coordination polymerization processes. TMVS was found to undergo migratory-insertion into the Ti-Me bond to give the corresponding [Cp<sub>2</sub>TiCH<sub>2</sub>CHMe(SiMe<sub>3</sub>)]<sup>+</sup> (III) which, in contrast to II, exists as an equilibrating mixture of a γ-agostic species (type C) and a higher energy β-agostomer (type B).

In addition to these differences in agostic behavior, II and III, both also exhibited major differences in modes of inter- and intramolecular hydrogen exchange processes. For instance, II and II-CD<sub>3</sub> ([Cp<sub>2</sub>TiCH<sub>2</sub>CH(CD<sub>3</sub>)(CMe<sub>3</sub>)]<sup>+</sup>) undergo reversible, intramolecular H-H(D) random exchange processes between the α-, β-, and γ (β-Me)-positions of the alkyl ligands in addition to concomitant intermolecular H-H(D) exchange with the vinylic and 2-methyl sites of the product of β-hydrogen elimination, CH<sub>2</sub>=CMeCMe<sub>3</sub>.<sup>4b,d</sup> In contrast, III undergoes tunnelling-expedited exchange of the hydrogen atoms of the β-methyl group with the β-H but not with either of the α-H sites (β-H/γ-H exchange), while III-CD<sub>3</sub> ([Cp<sub>2</sub>TiCH<sub>2</sub>CH(CD<sub>3</sub>)(SiMe<sub>3</sub>)]<sup>+</sup>) isomerizes specifically to the isotopomer [Cp<sub>2</sub>TiCD<sub>2</sub>CD(CH<sub>3</sub>)(SiMe<sub>3</sub>)]<sup>+</sup>, forgoing β-H/γ-H exchange completely.<sup>4c</sup>

Given the huge differences in behavior between the seemingly very similar complexes II and III and their CD<sub>3</sub> analogues, we have extended our studies to the sterically very hindered alkene triethylvinylsilane, TEVS, which also seems to be too sterically hindered to polymerize via a coordination polymerization process.<sup>6</sup> We find that TEVS reacts with I to give the anticipated product of 1,2-insertion, [Cp<sub>2</sub>TiCH<sub>2</sub>CHMe(SiEt<sub>3</sub>)]<sup>+</sup> (IV) and that this, as expected by analogy with III, is γ-agostic. Interestingly, however, IV is found

Received: August 4, 2015

Published: October 28, 2015

to isomerize, via an intramolecular 1,5- $\sigma$  bond metathesis process involving  $\varepsilon$ -agostic interactions to the alkyl complex  $[\text{Cp}_2\text{TiCH}_2\text{CH}_2(\text{SiEt}_2\text{CHMe}_2)]^+$  (V). In V, a close Ti–C( $\beta$ ) contact is stabilized by a strong  $\gamma$ -silyl interaction, and it is this latter behavior, not possible for III, which will be examined most closely in this article. For purposes of clarification in the discussion, we show the structures of complexes I to V in Figure 1.

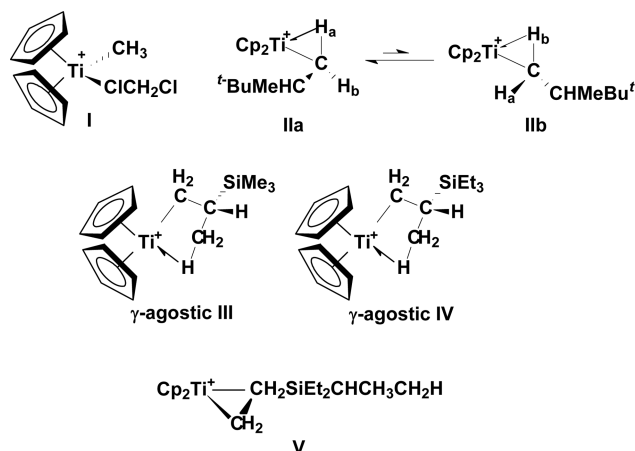


Figure 1. Structures of complexes I–V.

## EXPERIMENTAL SECTION

All syntheses were carried out utilizing an MBraun Labmaster glovebox under  $\text{N}_2$  or standard Schlenk line techniques with argon deoxygenated by passage through a heated column of BASF copper catalyst and then dried by passing through a column of activated 4A molecular sieves. NMR spectra were recorded using a Bruker AV600 spectrometer,  $^1\text{H}$  and  $^{13}\text{C}$  NMR data being referenced to TMS via the residual proton signals of the solvent. Details of the chemical shift and coupling constant data were gleaned from COSY and NOESY experiments and  $^{13}\text{C}$  data from HSQC and HMBC experiments (Supporting Information, Figures S2–S5).  $[\text{Ph}_3\text{C}][\text{B}(\text{C}_6\text{F}_5)_4]$  was purchased from Asahi Glass Company and used as obtained, while  $\text{CH}_3\text{Li}$ ,  $\text{CD}_3\text{Li}$ , and TEVS were purchased from Sigma-Aldrich.  $\text{Cp}_2\text{TiMe}_2$  was synthesized from  $\text{Cp}_2\text{TiCl}_2$  and  $\text{CH}_3\text{Li}$ , as described previously,<sup>4</sup> and was stored in ethyl ether solution ( $\sim 40.5$  mM) under argon at  $-30$  °C. Dichloromethane- $d_2$  was dried by storage over activated 3A molecular sieves.

Solutions containing  $[\text{Cp}_2\text{Ti}(\text{Me})(\text{CD}_2\text{Cl}_2)][\text{B}(\text{C}_6\text{F}_5)_4]$  (I) for NMR studies were prepared in  $\text{CD}_2\text{Cl}_2$  as previously reported.<sup>4c,d</sup> After a spectrum of I was obtained at 205 K, the tube was removed from the probe to a dry ice/acetone bath (195 K) and aliquots of TEVS (molar ratio I/alkene  $\approx 1:0.5$  to  $1:1.1$ ) were added. The tube was carefully shaken at 195 K to induce mixing and placed back in the probe at 205 K at which temperature the resonances of I were replaced within minutes by those of IV. A typical  $^1\text{H}$  NMR spectrum of IV is shown in Figure 2, while relevant COSY, HSQC, HMBC, and NOESY experiments are shown in Figures S2–S5. Note that although solutions of IV prepared as described above always contained relatively small amounts of the contact ion pair  $[\text{Cp}_2\text{TiMe}\{\text{B}(\text{C}_6\text{F}_5)_4\}]$ ,<sup>4a</sup> the latter did not react with TEVS under the experimental conditions used here. As is described in more detail below, holding an NMR sample much above about 245 K resulted in line broadening, presumably because of the formation of Ti(III) species.

The deuterium labeled compound IV- $\text{CD}_3$  was prepared by the reaction of  $[\text{Cp}_2\text{Ti}(\text{CD}_3)(\text{CD}_2\text{Cl}_2)][\text{B}(\text{C}_6\text{F}_5)_4]$  (I- $\text{CD}_3$ )<sup>4c,d</sup> with TEVS. NMR solutions of IV- $\text{CD}_3$  were prepared as described above for IV, and  $^1\text{H}$  NMR spectra were typically very similar to those of IV except for the absence of the resonance of the  $\beta$ -Me group.

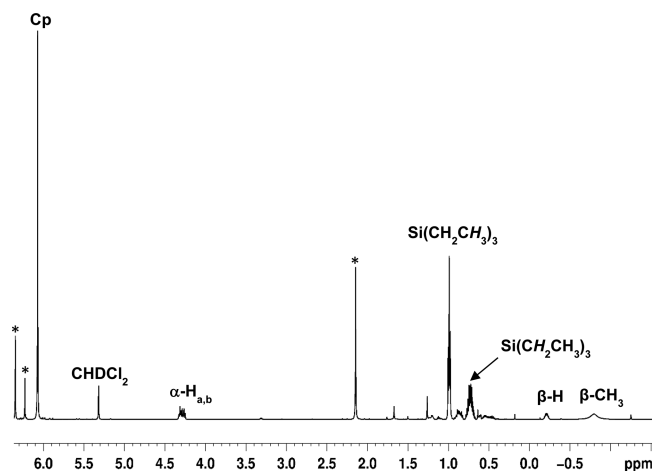


Figure 2.  $^1\text{H}$  NMR spectrum of IV in  $\text{CD}_2\text{Cl}_2$  at 225 K (\* =  $\text{Ph}_3\text{CMe}$ ).

In cases where we wished to monitor the conversion of IV to other species over relatively long periods of time, the NMR tube containing a sample of IV was transported from the NMR spectrometer in a dry ice/acetone bath to the cooling coil of a Neslab CC100 immersion cooler maintained at 235 K. The NMR tube was maintained under a flow of Ar and allowed to react at 235 K for  $\sim 30$  h.

The Geometry optimizations were carried out with Turbomole<sup>7a,b</sup> using the TZVP basis<sup>7c</sup> and the TPSSH functional<sup>7d</sup> (without RI approximation) in combination with an external optimizer (PQS OPTIMIZE).<sup>7e,f</sup> Vibrational analyses were carried out for all stationary points to confirm their nature (1 imaginary frequency for transition states, none for minima). Final energies were obtained using Gaussian 03,<sup>8a</sup> the M06-2X functional<sup>8b</sup> (which works well for olefin insertion<sup>8c</sup>), and the aug-cc-pVTZ basis set<sup>8d-g</sup> obtained from the EMSL basis set library.<sup>8h,i</sup>

To account for the reduced freedom of movement in solution, entropy contributions to the free energies were scaled to 2/3 of their gas-phase values,<sup>9a,b</sup> but no specific solvent corrections were applied. Calculated total energies for all relevant species and transition states may be found in the Table S1; geometries are provided as an xyz archive.

The potential-energy surface connecting various isomeric agostic structures is relatively flat. Because of the combination of thermal corrections and improved single-point energies, it occasionally happens that the calculated final free energy of a transition state for a rearrangement ends up lower in energy than the reactant (or product). This is not an error, but usually indicates that the reactant structure does not correspond to a local minimum on the free-energy surface. NMR parameters (chemical shifts and coupling constants) were calculated using Gaussian 03,<sup>8a</sup> the GIAO method,<sup>9c,d</sup> the TPSSH functional,<sup>7d</sup> and the IGLO-II basis set<sup>10a</sup> (TZVP basis on Ti<sup>7c</sup>). NMR simulations were carried out using gNMR V5.1.<sup>10b</sup>

The  $\text{SiEt}_3$  and  $\text{SiEt}_2\text{iPr}$  groups have considerable conformational freedom, and an exhaustive search of all possible silyl group conformations for each agostic structure was not possible. For most species, we tried several plausible-looking starting geometries, based on fully optimized smaller model systems; in the text, we only refer to the most stable variation found for each species.

## RESULTS AND DISCUSSION

**Synthesis and Structural Characterization of  $[\text{Cp}_2\text{TiCH}_2\text{CHMe}(\text{SiEt}_3)]^+$  (IV) and of  $[\text{Cp}_2\text{TiCH}_2\text{CHCD}_3(\text{SiEt}_3)]^+$  (IV- $\text{CD}_3$ ).** The species obtained in reactions of  $\text{Cp}_2\text{TiMe}_2$  with a slight excess of  $[\text{Ph}_3\text{C}][\text{B}(\text{C}_6\text{F}_5)_4]$  have been described previously.<sup>4</sup> In addition to  $\text{Ph}_3\text{CMe}$ , the product of methyl carbanion abstraction, mixtures of the solvent separated, ionic  $[\text{Cp}_2\text{Ti}(\text{Me})(\text{CD}_2\text{Cl}_2)][\text{B}(\text{C}_6\text{F}_5)_4]$  (I, major product),

and the contact ion pair  $[\text{Cp}_2\text{TiMe}\{\text{B}(\text{C}_6\text{F}_5)_4\}]$  (minor product) are formed, and it is the former which reacts with alkenes. NMR samples containing **I** were prepared as described in the [Experimental Section](#) and were placed in the probe of a 600 MHz NMR spectrometer preset to 205 K. The  $^1\text{H}$  NMR spectra were found to exhibit resonances of the products:  $\text{CMePh}_3$  at  $\delta$  7.0–7.3 (m), 2.13 (s); **I** at  $\delta$  6.72 (Cp), 1.63 (Me);  $[\text{Cp}_2\text{TiMe}\{\text{B}(\text{C}_6\text{F}_5)_4\}]$  at  $\delta$  6.33 (Cp), 1.24 (Me).

The addition of one equivalent of TEVS to a solution of **I** in  $\text{CD}_2\text{Cl}_2$  at 195 K resulted in a rapid reaction in which the resonances of **I** were replaced by resonances of a new species, **IV**. As is seen in [Figure 2](#), a  $^1\text{H}$  NMR spectrum of **IV** at 225 K exhibits a singlet at  $\delta$  6.07 (10H), a multiplet at  $\delta \sim 4.3$  (2H), a triplet at  $\delta$  0.99 (9H), a multiplet at  $\delta \sim 0.73$  (6H), a multiplet at  $\delta -0.21$  (1H), and a broad resonance at  $\delta -0.80$  (3H). On the basis of these spectral data and obvious spectral similarities with those of **III** ([Table 1](#)), **IV** is identified as

**Table 1.** NMR Data for **IV** at 225 K<sup>a</sup>

group	$^1\text{H}$ ( $\delta$ )	$^{13}\text{C}$ ( $\delta$ )	$J_{\text{HH}}$
$\alpha\text{-H}_a$	4.32 (4.81)	101.1 (100.0), $^1J_{\text{CH}}$ 152	$^2J_{\text{HH}}$ 9.0 (−9.7), $^3J_{\text{HH}}$ 7.8 (8.3)
	4.41 (4.78)	102.9 (107.5), $^1J_{\text{CH}}$ 150 (148.3)	$^2J_{\text{HH}}$ 8.9, $^3J_{\text{HH}}$ 7.8
$\alpha\text{-H}_b$	4.27 (4.22)	101.1 (100.0) $^1J_{\text{CH}}$ 147	$^2J_{\text{HH}}$ 9.0 (−9.7), $^3J_{\text{HH}}$ 13.1 (13.9)
	4.31 (4.77)	102.9 (107.5), $^1J_{\text{CH}}$ 147 (142.7)	$^2J_{\text{HH}}$ 8.9, $^3J_{\text{HH}}$ 12.6
$\beta\text{-H}$	−0.21 (−0.23)	−5.6 (−0.4), $^1J_{\text{CH}}$ 138	$^3J_{\text{HH}}$ 12.6, 7.8, 6.9
	−0.36 (0.03)	−1.8 (7.7), $^1J_{\text{CH}}$ 133 (124.5)	$^3J_{\text{HH}}$ 12.6, 7.8, 6.9
$\beta\text{-Me}$	−0.80 (−1.05)	33.7 (39.0)	$^3J_{\text{HH}}$ 6.9 (7.5)
	−0.78 (−0.94)	34.0 (34.2)	$^3J_{\text{HH}}$ 6.9
$\text{CH}_2$ of $\text{Et}_3\text{Si}^b$	$\delta$ 0.71, 0.75	2.9, $^1J_{\text{CH}} \sim 124$	$^2J_{\text{HH}}$ 15.4, $^3J_{\text{HH}}$ 7.8, 7.9
$\text{CH}_3$ of $\text{Et}_3\text{Si}^b$	0.99	6.6, $^1J_{\text{CH}}$ 126	
Cp	6.07	111.9, $^1J_{\text{CH}}$ 178	
	6.07	112.3	

<sup>a</sup>Data in parentheses are values calculated for the  $\gamma$ -agostomer, while analogous experimental and selected computed data for **III** are in italics. <sup>b</sup> $J$  was determined at 250 K.

$[\text{Cp}_2\text{TiCH}_2\text{CHMe}(\text{SiEt}_3)]^+$ , the product of a single 1,2-insertion of TEVS into the Ti–Me bond of **I** ([Scheme 1](#); for reasons of simplicity, we show the nonagostic isomer).

**Scheme 1.** Formation of **IV**



Thus the 9H ( $\delta$  0.99 (t)) and the 10H ( $\delta$  6.07 (s)) resonances are attributed to the  $\text{SiEt}_3$  methyl and the Cp groups, respectively, and the multiplet at  $\delta \sim 4.3$  is assigned to the  $\alpha\text{-H}$  atoms. The latter separates at 225 K into the A and B components of an ABX spin system at  $\delta$  4.31 and 4.27 ( $X = \beta\text{-H}$  at  $\delta -0.21$ ), and these diverge further to broadened resonances at  $\delta$  4.33 and 4.18 on cooling to 172 K.<sup>11a</sup> Careful analysis of these resonances at 225 K, using gNMR

simulations,<sup>10b</sup> resulted in chemical shifts of  $\delta$  4.32 and 4.27 and coupling constants  $^2J_{\alpha\alpha}$  9.0 Hz,  $^3J_{\alpha\beta}$  7.8, 13.1 Hz, and  $^3J_{\beta\gamma(\text{av})}$  7.0 Hz. The 6H multiplet at  $\delta \sim 0.73$  is assigned to the methylene hydrogens of the  $\text{SiEt}_3$  group and the broad 3H resonance at  $\delta -0.80$  to the three hydrogen atoms of the  $\beta\text{-Me}$  group.

Also relating **IV** to **III**, the  $\beta\text{-Me}$  resonance became much sharper at 235 K but decoalesced in the range 200–170 K to give a 1H resonance at  $\delta -7.3$  which is assigned to the  $\gamma$ -agostic hydrogen atom. A similar observation was made previously with  $\gamma$ -agostic **III**,<sup>4c</sup> and the observed broadening of the  $\beta\text{-Me}$  resonance as the temperature was lowered and its decoalescence at very low temperatures are consistent once again with a  $\gamma$ -agostic interaction which significantly increases the methyl rotational barrier. All assignments are shown in [Table 1](#) where they are compared with data for **III**. Consistent with the expected similarities in structures of **III** and **IV**, there are clearly quite pronounced similarities in the  $^1\text{H}$  and  $^{13}\text{C}$  spectral parameters for the  $\alpha\text{-CH}_2$ , the  $\beta\text{-CH}$ , the  $\beta\text{-Me}$ , and the Cp groups of the two complexes. Also, given the negative chemical shifts of both the  $\beta$ - and the (decoalesced)  $\gamma\text{-H}$  resonances, it would seem that there are agostic contributions to both, again as with **III**.

As mentioned above, **II**<sup>4d</sup> and **III**<sup>4c</sup> and their  $\text{CD}_3$  analogues undergo a variety of unusual exchange processes, and we began our investigation of **IV** with a view to extending the previous studies. During the course of this work, which continues and will be reported when completed, we observed the quite unanticipated rearrangement of **IV** and  $\text{IV-CD}_3$  to a new species **V**, and it is this process and the product formed which we discuss now.

**Formation and Structural Characterization of  $[\text{Cp}_2\text{TiCH}_2\text{CHMe}(\text{SiEt}_3)]^+$  (**V**).** On holding an NMR sample of **IV** or  $\text{IV-CD}_3$  for several hours at 235 K, there slowly evolved a new Cp resonance at  $\delta$  6.84, henceforth attributed to the new species **V**. As the resonance at  $\delta$  6.84 developed, the Cp resonances of **IV** or  $\text{IV-CD}_3$  weakened and disappeared, and after a sample had been held at 235 K for 25 h, the new resonance was found to be essentially the only Cp resonance remaining in the spectrum ([Figure 3](#)). A NOESY spectrum at this point exhibited correlations between the new Cp resonance at  $\delta$  6.84 with multiplets at  $\delta$  4.30, 0.99, 0.93, 0.80, and  $-0.40$  ([Figure S7](#)), and a  $^1\text{H-}^{29}\text{Si}$  HMBC experiment showed that all

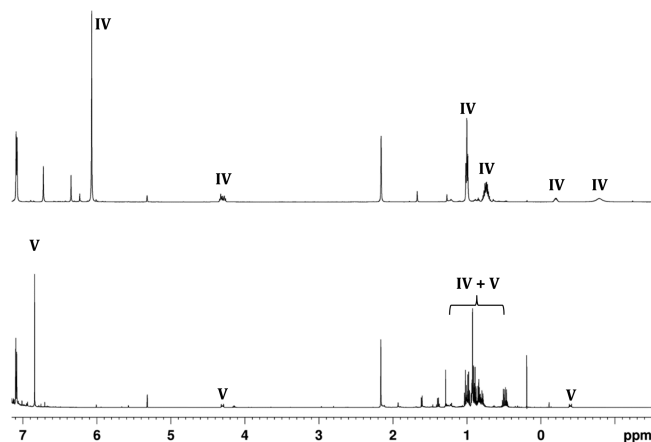


**Figure 3.**  $^1\text{H}$  NMR spectra ( $\text{CD}_2\text{Cl}_2$ ) of an NMR sample held at 235 K. The upper spectrum is of **IV** at 0 h; the lower spectrum shows the appearance of **V** after 25.5 h.



of these resonances correlated with a single  $^{29}\text{Si}$  resonance at  $\delta$  28.4, confirming that all belonged to the same molecule. The  $^1\text{H}$ - $^{29}\text{Si}$  HMBC experiment also showed the unfortunate presence of other compounds, presumably silicon containing byproducts of the formation of **V**, and their  $^1\text{H}$  resonances contributed greatly to the complexity of the  $^1\text{H}$  resonances in the region  $\delta$  0.3–1.5. As a result, the three resonances of **V** at  $\delta$  0.99, 0.93, and 0.80 were partially obscured and could not be satisfactorily viewed directly (see below).

In contrast, those at  $\delta$  4.30 (2H) and  $-0.40$  (2H) were well separated from all other resonances and were found to exhibit the unusual multiplet structures shown in Figure 4.

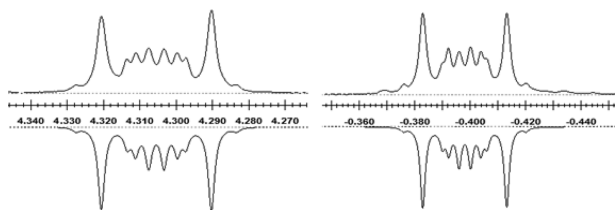


**Figure 4.** Resonances of **V** at  $\delta$   $-0.40$  and  $4.30$  (upper spectra) and simulated spectra for an AA'XX' spin system (bottom, inverted) with  $^2J_{\text{HH}}$  5.3, 6.7 Hz,  $^3J_{\text{HH}}$  5.0, 13.2 Hz.

Interestingly, the multiplet structures were identical whether the sample was derived from **IV** or **IV-CD**<sub>3</sub>, and thus neither site contained a deuterium atom! Furthermore, the two resonances exhibited only mutual COSY correlations, none with other resonances in the molecule.

We note at this point that the chemical shifts of the Cp ( $\delta$  6.84) and two apparent CH<sub>2</sub> groups ( $\delta$  4.30,  $-0.40$ ) of **V** are very similar to the chemical shifts of, respectively, the Cp ( $\delta$  6.87, s),  $\alpha$ -CH<sub>2</sub> ( $\delta$  4.19, br t), and  $\beta$ -CH<sub>2</sub> ( $\delta$   $-0.62$ , br t) resonances of the previously reported  $[\text{Cp}_2\text{TiCH}_2\text{CH}_2\text{CMe}_3]^+$ ,<sup>4b,d</sup> suggesting a possible similarity in structure with  $\alpha$ - and  $\beta$ -CH<sub>2</sub> groups and presumably a  $\beta$ -trialkylsilyl group of some kind. The complex  $[\text{Cp}_2\text{TiCH}_2\text{CH}_2\text{CMe}_3]^+$  assumes a conventional  $\beta$ -agostic structure in which the two  $\beta$ -H atoms take part in a rapid, degenerate exchange between agostic and nonagostic positions with the result that the time averaged chemical shift of the  $\beta$ -H atoms has a negative value. The resulting  $\alpha$ -H<sub>2</sub> and  $\beta$ -CH<sub>2</sub> resonances constitute an AA'XX' spin system,<sup>10c</sup> and both have the appearance of broadened 1:2:1 triplets in which  $J_{\text{AX}} \approx J_{\text{AX}}'$ ; apparent  $^3J_{\text{HH}}$  values are 7.7 Hz.<sup>4b,d</sup>

As is shown in Figure 4, however, the resonances at  $\delta$  4.30 and  $-0.40$  are not the pair of triplets which one would anticipate on the basis of the spectral data for  $[\text{Cp}_2\text{TiCH}_2\text{CH}_2\text{CMe}_3]^+$ . Instead, although the two complex multiplet resonances are simulated very satisfactory as the components of an AA'XX' spin system, quite clearly the  $J$  couplings of **V** are very different from those of **IV** and suggest a very different mode of bonding (see below).

While the complexity of the 1D  $^1\text{H}$  NMR spectrum in the region  $\delta$  0.3–1.5 made identification and analysis of the resonances of **V** difficult, observation of NOE correlations of the resonances at  $\delta$  4.30 and  $-0.40$  with three resonances, at  $\delta$  0.99, 0.93, and 0.80, strongly imply that the original SiEt<sub>3</sub> moiety was no longer intact and that **V** contained a more complex trialkylsilyl group. A high resolution NOESY experiment with **V-CD**<sub>3</sub> was useful in assigning the resonances, and a horizontal trace of the NOESY experiment at the  $\beta$ -H

resonance (Figure S8) made it possible to determine their multiplicities: a triplet at  $\delta$  0.99 ( $J \sim 7.7$  Hz), a doublet at  $\delta$  0.93 ( $J \sim 6.9$  Hz), and a multiplet at  $\delta \sim 0.80$ . A high resolution COSY experiment (Figure S9) exhibited correlations between the triplet at  $\delta$  0.99 and the multiplet at  $\delta \sim 0.80$ , and between the doublet at  $\delta$  0.93 and a multiplet at  $\delta \sim 1.0$ , which is obscured by the triplet at  $\delta$  0.99.

Thus, the spectral data are consistent with the presence of a SiEt<sub>2</sub>CHMe<sub>2</sub> group, the triplet, and multiplet at  $\delta$  0.99 and  $\sim 0.80$ , respectively, being attributable to the ethyl groups, the doublet and obscured multiplet at  $\delta$  0.93 and  $\sim 1.0$  to the isopropyl group. The CH<sub>2</sub> H atoms of the SiEt<sub>2</sub>CHMe<sub>2</sub> group are magnetically inequivalent in this structure, and thus their resonance is not a 1:3:3:1 quartet but rather a double quartet, providing inferential evidence of the presence of an SiEt<sub>2</sub> rather than an SiEt<sub>3</sub> moiety in the molecule. NMR data for **V** are presented in Table 2, those for  $^{13}\text{C}$  being derived from HSQC and HMBC experiments (Figures S10 and S11).

**Table 2.** NMR Data for **V** at 235 K<sup>a</sup>

group	$^1\text{H}$ ( $\delta$ )	$^{13}\text{C}$ ( $\delta$ , $^1J_{\text{CH}}$ Hz)	$J_{\text{HH}}$
$\alpha$ -CH <sub>2</sub>	4.30 (4.63)	98.3 (94.5), $^1J_{\text{CH}}$ 152	$^2J_{\text{HH}}$ ( $\alpha$ -CH <sub>2</sub> ) 5.3 ( $-6.6$ ), $^3J_{\text{HH}}$ ( $\alpha$ -CH <sub>2</sub> / $\beta$ -CH <sub>2</sub> ) 5.0, 13.2 (5.1, 13.5)
$\beta$ -CH <sub>2</sub>	$-0.40$ ( $-0.60$ )	17.0 (31.2), $^1J_{\text{CH}}$ 115	$^2J_{\text{HH}}$ ( $\beta$ -CH <sub>2</sub> ) 6.7 ( $-6.0$ )
CH	$\sim 1.00$	11.7, $^1J_{\text{CH}} \sim 120$	$^3J_{\text{HH}}$ 7.1
C(CH <sub>3</sub> ) <sub>2</sub>	0.93	16.7, $^1J_{\text{CH}}$ 127	$^3J_{\text{HH}}$ 7.1
CH <sub>2</sub> of Et <sub>3</sub> Si	0.805	2.6, $^1J_{\text{CH}} \sim 120$	$^3J_{\text{HH}}$ 7.7
CH <sub>3</sub> of Et <sub>3</sub> Si	0.99	6.7, $^1J_{\text{CH}}$ 126	$^3J_{\text{HH}}$ 7.7
Cp	6.84	120.1, $^1J_{\text{CH}}$ 175	

<sup>a</sup>Data in parentheses are values calculated for the low energy structure of **V** (see below).

We have noted above that the  $^1\text{H}$  NMR spectral data for **V** and  $[\text{Cp}_2\text{TiCH}_2\text{CH}_2\text{CMe}_3]^+$  suggest a similarity in structure. We note now that  $^{13}\text{C}$  data for  $[\text{Cp}_2\text{TiCH}_2\text{CH}_2\text{CMe}_3]^+$  are as follows:  $\delta$  94.6 ( $\alpha$ -C,  $^1J_{\text{CH}}$  146 Hz), 55.8 ( $\beta$ -C,  $^1J_{\text{CH}}$  116 Hz), 28.8 (Me,  $^1J_{\text{CH}}$  126 Hz), 37.9 (quaternary C), and 120.5 (Cp,  $^1J_{\text{CH}}$  178 Hz). Thus, while the chemical shift and coupling data for the  $\alpha$ -C and Cp carbon atoms are very similar, those of the  $\beta$ -C atoms are very different, consistent with a significant difference in structure.

To our knowledge, the most relevant group 4 metal precedents for similar organometallic species exhibiting spectra indicative of AA'XX' spin systems are zirconocene complexes of the type  $[(\eta^5\text{-C}_5\text{H}_4\text{Me})_2\text{Zr}(\text{CH}_2\text{CH}_2\text{R})\text{L}]^+$  (R = Me, Et, Ph, CMe<sub>3</sub>, SiMe<sub>3</sub>; L = THF, PMe<sub>3</sub>), reported many years ago by Jordan et al.<sup>3b,c</sup> In these, the all-carbon alkyl complexes containing coordinated THF are nonagostic, as indicated by  $\beta$ -H resonances which are downfield of the corresponding  $\alpha$ -H resonances, while those containing PMe<sub>3</sub> are  $\beta$ -agostic with  $\beta$ -H resonances exhibiting negative chemical shifts, upfield of the corresponding  $\alpha$ -H resonances. The agostic complexes also exhibit  $^{13}\text{C}$  chemical shifts and  $^1J_{\text{CH}}$  values consistent with the apparent structures, and  $\beta$ -agostic  $[(\eta^5\text{-C}_5\text{H}_4\text{Me})_2\text{Zr}(\text{CH}_2\text{CHDCMe}_3)(\text{PMe}_3)]^+$  exhibits a substantial, temperature-dependent isotopic perturbation of resonance (IPR) in

the case of the  $\beta$ -CHD analogue, also supporting the presence of agostic H atoms.

In stark contrast, while the  $\beta$ -H resonance of  $[\text{Cp}_2\text{ZrCH}_2\text{CH}_2\text{SiMe}_3(\text{THF})]^+$  exhibited a negative chemical shift, the  $\beta$ -CHD analogue did not exhibit a temperature-dependent IPR. In addition, the chemical shift of the  $\beta$ -C atom and the  $^1J_{\text{CH}}$  values of the  $\alpha$ - and the  $\beta$ -C atoms all seemed anomalous, and recourse was made to an X-ray structural determination of  $[\text{Cp}_2\text{Zr}(\text{CH}_2\text{CH}_2\text{SiMe}_3)(\text{THF})][\text{BPh}_4]$ . This showed that there was a sufficiently close  $\text{Zr}-\text{C}(\beta)$  contact that the alkyl ligand was extremely distorted such that the  $\text{Zr}-\text{C}(\alpha)-\text{C}(\beta)$  bond angle was  $\sim 84^\circ$ . In addition, the  $\text{SiMe}_3$  group was found to lie in the  $\text{O}-\text{Zr}-\text{C}(\alpha)-\text{C}(\beta)$  plane, implying an absence of significant agostic  $\beta$ -H interactions with the metal. The molecule was therefore suggested to contain an agostic-like  $\text{Zr}\leftarrow\text{C}(\beta)-\text{Si}$  bonding interaction which was rationalized on the basis of a strong, trimethylsilyl-induced bonding interaction ( $\gamma$ -silyl effect) between the zirconium and the back lobe of the  $\beta$ - $\text{CH}_2$  group of the alkyl ligand as in Figure 5.<sup>3d</sup> This unusual mode of bonding was thought to be analogous to that postulated as a  $\gamma$ -silyl effect for analogous silyl carbenes and carbocations.<sup>12</sup>

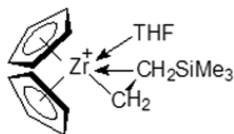


Figure 5. Structure of  $[(\eta^5\text{-C}_5\text{H}_4\text{Me})_2\text{Zr}(\text{CH}_2\text{CH}_2\text{SiMe}_3)(\text{THF})]^+$ .<sup>3d</sup>

Chemical shift data for the complexes  $[(\eta^5\text{-C}_5\text{H}_4\text{Me})_2\text{Zr}(\text{CH}_2\text{CH}_2\text{SiMe}_3)\text{L}]^+$  ( $\text{L} = \text{THF}, \text{PMe}_3$ ) are similar to those of **V**, the  $\text{ZrCH}_2$  and  $\text{CH}_2\text{SiMe}_3$  chemical shifts being in the ranges  $\delta$  1 to 1.8 and  $-2.15$  to  $0.71$ , respectively, and thus consistent with similarities in structure. However, the second order AA'XX' multiplets of the zirconium complexes were not analyzed and thus comparisons with the coupling data for **V** cannot be made.

**Computational Studies on IV and V.** In an effort to better understand the structures of **IV** and **V** and the nature of the isomerization process, a number of structures for the two complexes were explored by DFT methods. The relative energies of the most important of the species considered, relative to the  $\gamma$ -agostomer of **IV** set to zero, are summarized in the upper half of Figure 6 for **IV**, with those of **V** in the lower half. Note that conclusions based on the computational studies agreed in considerable detail with those based on the experimental results.

For the initial insertion product **IV**, we located  $\alpha$ -H,  $\beta$ -H,  $\gamma$ -H,  $\delta$ -H, and  $\epsilon$ -H agostic structures as well as local minima where the  $\beta$ -C- $\gamma$ -Si bond interacts with the metal center ("Si-agostic").<sup>2s-v</sup> Except for the lowest-energy structure, all of these are kinetically irrelevant as interconversion happens well below the rearrangement transition state. (Interactions with  $\beta$ -C- $\gamma$ -Si bonds are not as common, presumably because in most cases  $\beta$ -H or  $\gamma$ -H agostic structures are preferred, as they are in the present case.)

As with **III**,<sup>4c</sup> we find that the preferred structure of **IV** is  $\gamma$ -agostic with a Ti-agostic H( $\gamma$ ) distance of  $1.975 \text{ \AA}$ , a C( $\gamma$ )-H( $\gamma$ ) bond distance of  $1.145 \text{ \AA}$  and a Ti-C( $\alpha$ )-C( $\beta$ ) bond angle of  $82.36^\circ$ . As shown in Figure 6, the  $\beta$ -agostomer of **IV** lies  $1.7 \text{ kcal/mol}$  above the  $\gamma$ -agostomer, followed by  $\epsilon$ - and  $\delta$ - (both

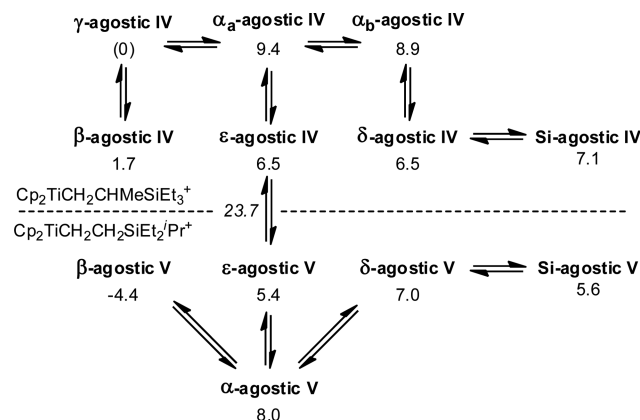


Figure 6. Calculated relative free energies (kcal/mol) of agostomers for **IV** and its rearrangement product **V**. The 23.7 in italics represents the transition state, relative to the  $\gamma$ -agostomer, for the overall rearrangement process of **IV** to **V** (see below).

$6.5 \text{ kcal/mol}$ ) and the two  $\alpha$ -agostic structures ( $8.9, 9.4 \text{ kcal/mol}$ ). For **III**, the energies of the  $\beta$ - and two  $\alpha$ -agostomers are, respectively,  $1.9 \text{ kcal/mol}$  and  $3.0, 4.2 \text{ kcal/mol}$ , and thus, while the  $\gamma$ - $\beta$  energy differences are very similar in the two complexes, the  $\gamma$ - $\alpha$  energy differences seem to be higher in **IV**, possibly because of greater steric hindrance although a somewhat different functional/basis set was used in our previous work.<sup>4c</sup>

While  $\beta$ -agostic structures are commonly preferred for alkyls bearing  $\beta$ -hydrogen atoms,<sup>5</sup> the relatively high energy of the  $\beta$ -agostic structure in this case is probably due to steric hindrance caused by the  $\beta$ -Me group which hinders the approach of the  $\beta$ -H atom in a favorable geometry. Similar observations of higher energy  $\beta$ -agostic structures have been made previously for **II** and **III**.<sup>4b-d</sup>

The isomerization product **V** can, in principal, assume  $\alpha$ -,  $\beta$ -,  $\delta$ -, and  $\epsilon$ -H agostic structures, and the relative energies of these species, relative to the  $\gamma$ -agostomer of **IV** set to zero, are summarized in the lower half of Figure 5. As is seen, the  $\alpha$ -,  $\delta$ -, and  $\epsilon$ -H agostomers all have energies within  $1\text{--}4 \text{ kcal/mol}$  of the corresponding agostomeric structures of **IV**, while the  $\beta$ -agostomer is lower by  $6.1 \text{ kcal/mol}$ . Indeed the latter is the global minimum of the system, and its formation provides a driving force of  $-4.4 \text{ kcal/mol}$  for the rearrangement. Somewhat surprisingly, however, the low energy  $\beta$ -agostomer is found to assume neither a conventional  $\beta$ -H agostic structure, in which solely a  $\beta$ -H atom interacts with the metal as in  $[\text{Cp}_2\text{TiCH}_2\text{CH}_2\text{CMe}_3]^+$ , nor a "central geometry" Jordan-type structure, as in Figures 1 and 5 in which a symmetric Ti-C( $\beta$ )-Si interaction is facilitated by a  $\gamma$ -silyl effect in the apparent absence of a  $\beta$ -H agostic interaction. Instead, the preferred, lowest energy orientation of **V** essentially has one of the  $\beta$ -H atoms and the carbon atom of the  $\beta$ - $\text{CH}_2$  group within bonding distances of the titanium atom.

We present on line 1 of Table 3 several key structural parameters calculated for **V**, the Ti-agostic H( $\beta$ ), Ti-C( $\alpha$ ), Ti-C( $\beta$ ), and C( $\beta$ )-H( $\beta$ ) bond lengths, the Ti-C( $\alpha$ )-C( $\beta$ ) bond angle, the Ti-C( $\alpha$ )-C( $\beta$ )-H( $\beta$ ) torsional angle, and the Ti-C( $\beta$ )/Ti-C( $\alpha$ ) bond length ratio. For purposes of comparison, we also present the corresponding data for the simple  $\beta$ -agostic ethyl analogue  $[\text{Cp}_2\text{TiCH}_2\text{CH}_3]^+$ , for the  $\beta$ -agostomer of **IV**, for those of the all-carbon,  $\beta$ -agostic  $[\text{Cp}_2\text{TiCH}_2\text{CHMeCMe}_3]^+$ , and  $[\text{Cp}_2\text{TiCH}_2\text{CH}_2\text{CMe}_3]^+$ , and for a previously reported,  $\beta$ -agostic  $[\text{Cp}_2\text{TiCH}_2\text{CHC}(\text{Me})-$

Table 3. Calculated Structural Parameters for  $\beta$ -Agostomers of Complexes of the Type  $[\text{Cp}_2\text{TiR}]^+$ 

line	R	Ti-C( $\alpha$ )-C( $\beta$ )-H( $\beta$ ) (deg)	Ti-H( $\beta$ ) (Å)	C( $\beta$ )-H( $\beta$ ) (Å)	Ti-C( $\alpha$ ) (Å), Ti-C( $\beta$ ) (Å)	Ti-C( $\beta$ )/Ti-C( $\alpha$ )	Ti-C( $\alpha$ )-C( $\beta$ ) (deg)
1	$\text{CH}_2\text{CH}_2\text{SiEt}_2\text{CHMe}_2$ (V)	34.7, -87.1	2.134, 2.793	1.090, 1.130	2.138 2.418	1.13	81.1
2	$\text{CH}_2\text{CH}_3$	$\pm 2.3$	1.982	1.157	2.141 2.447	1.14	82.4
3	$\text{CH}_2\text{CH}_2\text{CMe}_3$	18.0	2.007, 2.949	1.165, 1.090	2.150, 2.474	1.15	83.3
4	$\text{CH}_2\text{CHMeCMe}_3$	12.3	2.073	1.168	2.169, 2.580	1.19	87.1
5	$\text{CH}_2\text{CHMeSiEt}_3$ (IV)	14.5	2.049	1.158	2.163, 2.520	1.165	84.7
6	$\text{CH}_2\text{CHC}(\text{Me})\text{CH}_2\text{CHMe}_2$	2.0	1.990	1.175	2.157, 2.526	1.17	85.2

$\text{CH}_2\text{CHMe}_2]^+$  (the current data for the latter complex are slightly different from those reported previously<sup>4a</sup> because a somewhat different functional/basis set was used for all complexes in Table 3).

It is anticipated that the relatively uncluttered ethyl complex (line 2) would prefer a perfectly eclipsed  $\beta$ -agostic orientation, with a torsion angle  $\angle\text{Ti}-\text{C}(\alpha)-\text{C}(\beta)-\text{H}(\text{agostic})$  of  $0^\circ$ , and this is essentially what is found. However, a perfectly staggered Jordan-like structure for V would have  $\angle\text{Ti}-\text{C}(\alpha)-\text{C}(\beta)-\text{H} = 60^\circ$  for both  $\beta$ -H atoms and  $\angle\text{Ti}-\text{C}(\alpha)-\text{C}(\beta)-\text{Si} = 180^\circ$ . Thus, the calculated twist indicated on line 1 for the  $\text{H}(\beta)\text{C}(\beta)$ -agostic structure of V ( $34.7^\circ$ ) is roughly midway between perfectly eclipsed and staggered structures.

Looking to the other  $\beta$ -H monoagostic complexes (lines 3–6), we see that the steric pressures exerted by the introduction of  $\beta$ -alkyl groups induce relatively minor twisting away from the purely eclipsed positions but that these result only in a torsion angle of up to  $18.0^\circ$ , much less than that calculated for V and suggesting that the latter species is different in some fundamental sense.

Comparing the other structural parameters, we see that the Ti-agostic  $\text{H}(\beta)$  distance of V is only slightly longer than the range of the others while the  $\text{C}(\beta)$ -agostic  $\text{H}(\beta)$  distance of V is only slightly shorter than the corresponding data for the other complexes; both sets of data suggest a marginally weaker Ti-agostic H interaction in V. However, the difference between the Ti-C( $\alpha$ ) and Ti-C( $\beta$ ) distance, 13%, is lower than the differences of the other complexes (14–19%), while the Ti-C( $\alpha$ )-C( $\beta$ ) bond angle of V,  $81.1^\circ$ , is lower than those of the others ( $82.4$ – $85.2^\circ$ ); these data comparisons imply a somewhat stronger agostic interaction for V. We note parenthetically that the range of metal-C( $\alpha$ )-C( $\beta$ ) bond angles of a variety of nonagostic metal-ethyl complexes is in the range  $108$ – $126^\circ$ ,<sup>20</sup> much greater than any of the Ti-C( $\alpha$ )-C( $\beta$ ) bond angles shown in Table 3.

Further evidence for a Ti-C( $\beta$ )-Si( $\gamma$ ) interaction in V is indicated by a calculated elongation (nearly  $0.1$  Å) of the C( $\beta$ )-Si( $\gamma$ ) bond relative to the three remaining Si( $\gamma$ )-C( $\delta$ ) bonds, and also by the very low barrier of only  $0.4$  kcal/mol for exchange between the two equivalent  $\beta$ -agostic structures via a staggered transition state. In essence, the silyl group swings from close to one Cp to close to the other while the Ti-C( $\alpha$ )-C( $\beta$ ) arrangement remains more or less unchanged. The two  $\beta$ -H atoms move in concert accompanied by a somewhat limited rotation about the C( $\alpha$ )-C( $\beta$ ) bond. The calculated Ti-C( $\alpha$ )-C( $\beta$ )-H( $\beta$ ) torsional angles of the transition state during rotation are  $65.6$  and  $-64.0^\circ$ , while the two Ti-H( $\beta$ ) distances are a very similar ( $2.478$  and  $2.499$  Å). In addition, the two C( $\beta$ )-H( $\beta$ ) distances are nearly identical ( $1.097$  and  $1.099$  Å), the Ti-C( $\beta$ ) distance is only 12% longer than the Ti-C( $\alpha$ ) distance, and the Ti-C( $\alpha$ )-C( $\beta$ ) angle is only  $79.7^\circ$ . Thus, the

transition state is, as anticipated, very symmetric and also very similar to a pure Jordan structure.

Four different conformations of the  $\text{SiEt}_2\text{CHMe}_2$  group were taken into account in the calculations from which the NMR data in Table 2 were acquired, and the calculated NMR data in Table 2 are for the lowest energy of these. For most data, the agreement between experimental and calculated is very good, lending considerable support to our conclusions concerning the structure of V. For this reason, the difference in the experimental and calculated  $\beta$ -C chemical shifts ( $\delta$  17.0 vs  $\delta$  31.2, respectively) is, therefore, just a bit bothersome as this particular carbon atom is, of course, the single most unique aspect of the structure. However, the  $\beta$ -C chemical shift is very sensitive to the precise orientation of the  $\beta$ -agostic interaction, presumably because the Si back-lobe phenomenon allows a wide range of structures of comparable energies, and the other conformations investigated exhibit C( $\beta$ ) chemical shifts of  $\delta$  31.2, 22.0, 25.0, and 16.1.

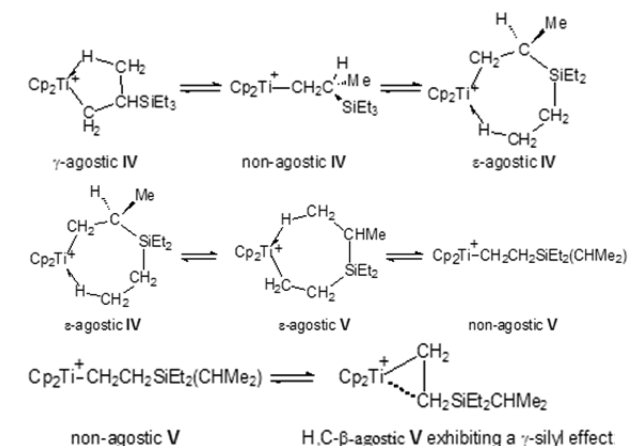
The last value is very similar to the experimental value, as are the other  $^1\text{H}$  and  $^{13}\text{C}$  chemical shifts of this conformation, and we have therefore taken a closer look at its structural parameters; the Ti-C( $\alpha$ )-C( $\beta$ )-H( $\beta$ ) torsional angles are  $53.4$  and  $-74.8^\circ$ , the Ti-H( $\beta$ ) distances are  $2.342$  and  $2.616$  Å, the C( $\beta$ )-H( $\beta$ ) distances are  $1.093$  and  $1.107$  Å, the Ti-C( $\beta$ ) distance is 12% longer than the Ti-C( $\alpha$ ) distance, and the Ti-C( $\alpha$ )-C( $\beta$ ) angle is  $80.1^\circ$ . Since the difference in energy between this conformation, which is considerably closer to the Jordan geometry, and that of the low energy structure of line 1 of Table 3 ( $1.5$  kcal/mol) is probably less than the error (uncertainties) of our computational methodology, it is possible that V does in fact assume this Jordan-like structure.

**Mechanism of Rearrangement of IV to V.** Since the apparent  $\text{CH}_2\text{CH}_2$  fragment of V contains no deuterium atoms, we can rule out its being derived from the alkyl ligands of IV or IV- $\text{CD}_3$  following any of the rearrangements discussed above for either these compounds or for III and III- $\text{CD}_3$ . Instead, it seems that only the  $\text{SiEt}_3$  group can be a candidate for the source of the  $\text{CH}_2\text{CH}_2$  fragment, and the conversion of IV to V therefore probably involves the 1,5  $\sigma$ -bond metathesis process shown in Scheme 2.

In this scenario, an  $\epsilon$ -agostic hydrogen atom migrates from a methyl group of one of the Si-bound ethyl groups to the original C( $\alpha$ ) of IV, forming  $\epsilon$ -agostic V. The latter can then rearrange to the species observed, containing a Ti-C( $\beta$ )-Si moiety stabilized by a  $\gamma$ -silyl effect. We have previously observed an analogous process in which the  $\sigma$ -alkyl complex  $[\text{Cp}_2\text{Ti}(\text{CH}_2\text{CMe}_2\text{CH}_2\text{CHMe}_2)]^+$  converts, via a 1,5  $\sigma$ -bond metathesis reaction involving two isomeric  $\epsilon$ -agostic species, to give the  $\sigma$ -alkyl species  $[\text{Cp}_2\text{Ti}(\text{CH}_2\text{CHMeCH}_2\text{CMe}_3)]^+$  which subsequently isomerizes to a lower energy  $\beta$ -agostic species.<sup>4a</sup> We note that the  $\epsilon$ -agostic methyl H atoms in question in both reactants are five bonds away from the metal, consistent with a



Scheme 2



1,5  $\sigma$ -bond metathesis reaction,<sup>4a</sup> and that both  $\sigma$ -bond metathesis reactions may be aided by the so-called Thorpe-Ingold effect.<sup>13</sup> It has long been known that the presence of *gem*-dimethyls on a carbon atom in an open carbon chain accelerates the rates and yields of cyclization processes involving the chain ends, a fact cited previously as mechanistic support in connection with the conversion of  $[\text{Cp}_2\text{Ti}(\text{CH}_2\text{CMe}_2\text{CH}_2\text{CHMe}_2)]^+$ , via a 1,5  $\sigma$ -bond metathesis reaction involving two isomeric  $\epsilon$ -agostic species, to  $[\text{Cp}_2\text{Ti}(\text{CH}_2\text{CHMeCH}_2\text{CMe}_2)]^+$ .<sup>4a</sup> We suggest that the presence of *gem*-diethyl groups on the silicon atom of IV is also likely to expedite the process observed, and we turned to DFT calculations to shed light on the mechanism of the rearrangement of IV to V.

The 1,5-hydrogen shift shown in Scheme 2 is similar to that which we reported previously for  $[\text{Cp}_2\text{Ti}(\text{CH}_2\text{CMe}_2\text{CH}_2\text{CHMe}_2)]^+$ ,<sup>4a</sup> and it occurs about 17.2 kcal/mol above the  $\epsilon$ -agostic structure, some 23.7 kcal/mol above the preferred  $\gamma$ -agostic structure. This rearrangement would therefore correspond to a relatively slow reaction in agreement with the experimental observations.

**Summary and Conclusions.** The complex  $[\text{Cp}_2\text{Ti}(\text{Me})(\text{CD}_2\text{Cl}_2)]^+$  (I) reacts with a variety of sterically encumbered alkenes to form monoinertion alkyl products exhibiting various kinds of agostic behavior,  $\alpha$ -,  $\beta$ -, and/or  $\gamma$ -, and this article describes the reaction of I with triethylvinylsilane (TEVS) which gives the  $\gamma$ -agostic  $\sigma$ -alkyl complex  $[\text{Cp}_2\text{Ti}(\text{CH}_2\text{CHMe}(\text{SiEt}_3))]^+$  (IV). Complex IV is of special interest because it undergoes a very unconventional intramolecular 1,5- $\sigma$  bond metathesis process in which a methyl group of one of the Si-bound ethyl groups forms a cyclic  $\epsilon$ -agostic species; the  $\epsilon$ -agostic hydrogen atom then migrates to the original C( $\alpha$ ) of IV, forming the isomeric,  $\epsilon$ -agostic  $[\text{Cp}_2\text{Ti}(\text{CH}_2\text{CH}_2(\text{SiEt}_2\text{CHMe}_2))]^+$  which rearranges to a more stable agostomer of  $[\text{Cp}_2\text{Ti}(\text{CH}_2\text{CH}_2(\text{SiEt}_2\text{CHMe}_2))]^+$  (V) which has been characterized by NMR spectroscopy and DFT calculations.

Complex V does not exhibit a conventional  $\alpha$ -,  $\beta$ -, or  $\gamma$ -H agostic structure but rather the type of structure found previously for the zirconium analogue  $[\text{Cp}_2\text{Zr}(\text{CH}_2\text{CH}_2\text{SiMe}_3)(\text{THF})]^+$ .<sup>3d</sup> The latter contains an unprecedented kind of  $\text{Zr} \leftarrow \text{C}(\beta)\text{-Si}$  ( $\beta$ -C agostic?) structure which was rationalized on the basis of a strong, trimethylsilyl-induced ( $\gamma$ -silyl effect<sup>12</sup>) bonding interaction between the zirconium and the back lobe of the  $\beta$ -CH<sub>2</sub> group of the alkyl ligand. Consistent with this hypothesis, the  $\text{SiMe}_3$  group was found to lie in the

$\text{O}-\text{Zr}-\text{C}(\alpha)-\text{C}(\beta)$  plane, suggesting the absence of significant agostic  $\beta$ -H interactions with the metal.<sup>3d</sup>

In an effort to better understand the structure of V, a number of structures were explored by DFT methods, and it was found that the lowest energy structure has one of the  $\beta$ -H atoms and the carbon atom of the  $\beta$ -CH<sub>2</sub> group within bonding distances of the titanium atom. It also has a  $\text{Ti}-\text{C}(\alpha)-\text{C}(\beta)$  of 81.1°, and thus, V also appears to contain an agostic-like  $\text{Zr} \leftarrow \text{C}(\beta)\text{-Si}$  bonding interaction, but one which is asymmetric because it is buttressed by a  $\beta$ -H agostic interaction. Complicating matters, however, we also find that the energy surface for interconversion of the two possible orientations in which the  $\beta$ -H atoms exchange is very flat and that the height of the barrier is well within the error of the calculations. In addition, a Jordan-like conformation with NMR parameters in substantially better agreement with the experimental data lies only 1.5 kcal/mol above that of the low energy structure of line 1 of Table 3, well within the error of the calculations. Thus we are left with a degree of uncertainty as to which structure really is of the lowest energy, and a Jordan-like, relatively symmetric structure may actually be the lowest energy agostomer in reality. Note that alternative  $\beta$ -agostic structures, containing a coordinated  $\text{CH}_2\text{Cl}_2$  à la Jordan, were also explored but that the  $\text{CH}_2\text{Cl}_2$  was found to dissociate spontaneously.

## ■ ASSOCIATED CONTENT

### Supporting Information

The Supporting Information is available free of charge on the ACS Publications website at DOI: 10.1021/acs.organomet.5b00675.

Figures and tables describing and elaborating on the NMR experiments; calculated energies for the  $\text{Cp}_2\text{TiCH}_3^+ + \text{TEVS}$  systems: b-p geometries, relative free energies and barriers, and calculated structures (PDF)

Computational information, additional structures, Cartesian coordinates of calculated species; computed Cartesian coordinates of all of the structures reported in this study; all structures have a name including the formula and the type of agostic interaction. Where there are different conformations, that of the lowest-energy has the original name (e.g.,  $\text{Cp}_2\text{TiCH}_2\text{CH}_2\text{SiEt}_2\text{iPr} + \text{AlpAgostic}$ ), and names of further conformations are followed by a number as in  $\text{Cp}_2\text{TiCH}_2\text{CH}_2\text{SiEt}_2\text{iPr} + \text{AlpAgostic2}$ . The file may be opened as a text file to read the coordinates or opened directly by a molecular modeling program such as Mercury (version 3.3, <http://www.ccdc.cam.ac.uk/pages/Home.aspx> for visualization and analysis (XYZ)

## ■ AUTHOR INFORMATION

### Corresponding Authors

\*(M.C.B.) E-mail: [bairdmc@chem.queensu.ca](mailto:bairdmc@chem.queensu.ca).

\*(P.H.M.B.) E-mail: [peter.budzelaar@umanitoba.ca](mailto:peter.budzelaar@umanitoba.ca).

### Notes

The authors declare no competing financial interest.

## ■ ACKNOWLEDGMENTS

M.C.B. gratefully acknowledges the Natural Science and Engineering Research Council of Canada (NSERC) and Queen's University for funding of this research. P.H.M.B. thanks the Natural Science and Engineering Research Council

of Canada, the Canada Foundation for Innovation, the Manitoba Research and Innovation Fund (CFI/MRIF Project 10831), and SABIC Petrochemicals Europe for financial support. A.D.-B. thanks Queen's University for a Carrel Graduate Fellowship.

## REFERENCES

- (1) For useful reviews of polymerization catalysis, see (a) Bochmann, M. J. *Chem. Soc., Dalton Trans.* **1996**, 255. (b) Resconi, L.; Camurati, I.; Sudmeijer, O. *Top. Catal.* **1999**, 7, 145. (c) Coates, G. W. *Chem. Rev.* **2000**, 100, 1223. (d) Resconi, L.; Cavallo, L.; Fait, A.; Piemontesi, F. *Chem. Rev.* **2000**, 100, 1253. (e) Chen, E. Y.-X.; Marks, T. J. *Chem. Rev.* **2000**, 100, 1391. (f) Rappé, A. K.; Skiff, W. M.; Casewit, C. J. *Chem. Rev.* **2000**, 100, 1435. (g) Bochmann, M. J. *Organomet. Chem.* **2004**, 689, 3982. (h) Fujita, T.; Makio, H. *Polymerization of Alkenes*; Comprehensive organometallic chemistry. Crabtree, R. H., Mingos, D. M. P., Eds.; Elsevier: Amsterdam, 2007; Vol. III, Chapter 11.20. (i) Froese, R. D. J. In *Computational Modeling for Homogeneous and Enzymatic Catalysis*; Morokuma, K.; Musaev, D. G., Eds.; Wiley-VCH: Weinheim, Germany, 2008; p 149. (j) Busico, V. *Macromol. Chem. Phys.* **2007**, 208, 26. (k) Wilson, P. A.; Hannant, M. H.; Wright, J. A.; Cannon, R. D.; Bochmann, M. *Macromol. Symp.* **2006**, 236, 100. (l) Alt, H. G.; Licht, E. H.; Licht, A. I.; Schneider, K. J. *Coord. Chem. Rev.* **2006**, 250, 2.
- (2) For reviews of agostic complexes, see (a) Brookhart, M.; Green, M. L. H. *J. Organomet. Chem.* **1983**, 250, 395. (b) Brookhart, M.; Green, M. L. H.; Wong, L.-L. *Prog. Inorg. Chem.* **1988**, 36, 1. (c) Grubbs, R. H.; Coates, G. W. *Acc. Chem. Res.* **1996**, 29, 85. (d) Scherer, W.; McGrady, G. S. *Chem. - Eur. J.* **2003**, 9, 6057. (e) Clot, E.; Eisenstein, O. *Struct. Bonding (Berlin, Ger.)* **2004**, 113, 1. (f) Scherer, W.; McGrady, G. S. *Angew. Chem., Int. Ed.* **2004**, 43, 1782. (g) Brookhart, M.; Green, M. L. H.; Parkin, G. *Proc. Natl. Acad. Sci. U. S. A.* **2007**, 104, 6908. (h) Lein, M. *Coord. Chem. Rev.* **2009**, 253, 625. For computational papers discussing the importance of  $\beta$ -agostic structures during metallocene-induced alkene polymerization, see (i) Lohrenz, J. C. W.; Woo, T. K.; Ziegler, T. *J. Am. Chem. Soc.* **1995**, 117, 12793. (j) Jensen, V. R.; Koley, D.; Jagadeesh, M. N.; Thiel, W. *Macromolecules* **2005**, 38, 10266. (k) Mitoraj, M. P.; Michalak, A.; Ziegler, T. *Organometallics* **2009**, 28, 3727. (l) Scherer, W.; Herz, V.; Hauf, C. *Struct. Bonding (Berlin, Ger.)* **2012**, 146, 159. (m) Laine, A.; Linnolahti, M.; Pakkanen, T. A.; Severn, J. R.; Kokko, E.; Pakkanen, A. *Organometallics* **2010**, 29, 1541. (n) Laine, A.; Linnolahti, M.; Pakkanen, T. A.; Severn, J. R.; Kokko, E.; Pakkanen, A. *Organometallics* **2011**, 30, 1350. (o) Dawoodi, Z.; Green, M. L. H.; Mtetwa, V.; Prout, K.; Schultz, A. J.; Williams, J. M.; Koetzle, T. F. *J. Chem. Soc., Dalton Trans.* **1986**, 1629. (p) Scherer, W.; Priemeier, T.; Haaland, A.; Volden, H. V.; McGrady, G. S.; Downs, A. J.; Boese, R.; Bläser, D. *Organometallics* **1998**, 17, 4406. For papers specifically describing late transition metal agostic complexes, see (q) Brookhart, M.; Lincoln, D. M.; Volpe, A. F.; Schmidt, G. F. *Organometallics* **1989**, 8, 1212. (r) Shultz, L. H.; Brookhart, M. *Organometallics* **2001**, 20, 3975. Interactions of  $\beta$ -Si- $\gamma$ -C bonds are well-documented; see, e.g., (s) Klooster, W. T.; Brammer, L.; Schaverien, C. J.; Budzelaar, P. H. M. *J. Am. Chem. Soc.* **1999**, 121, 1381. (t) Perrin, L.; Maron, L.; Eisenstein, O.; Lappert, M. F. *New J. Chem.* **2003**, 27, 121. (u) Stoebe, E. J.; Jordan, R. F. *J. Organomet. Chem.* **2006**, 691, 4956. (v) Beswick, C. L.; Marks, T. J. *Organometallics* **1999**, 18, 2410.
- (3) (a) Jordan, R. F.; Bradley, P. K.; Baenziger, N. C.; Lapointe, R. E. *J. Am. Chem. Soc.* **1990**, 112, 1289. (b) Alelyunas, Y. W.; Guo, Z.; Lapointe, R. E.; Jordan, R. F. *Organometallics* **1993**, 12, 544. (c) Alelyunas, Y. W.; Baenziger, N. C.; Bradley, P. K.; Jordan, R. F. *Organometallics* **1994**, 13, 148. (d) Guo, Z.; Swenson, D. C.; Jordan, R. F. *Organometallics* **1994**, 13, 1424.
- (4) (a) Sauriol, F.; Sonnenberg, J. F.; Chadder, S. J.; Dunlop-Brière, A. F.; Baird, M. C.; Budzelaar, P. H. M. *J. Am. Chem. Soc.* **2010**, 132, 13357. (b) Dunlop-Brière, A. F.; Baird, M. C.; Budzelaar, P. H. M. *Organometallics* **2012**, 31, 1591. (c) Dunlop-Brière, A. F.; Baird, M. C.; Budzelaar, P. H. M. *J. Am. Chem. Soc.* **2013**, 135, 17514. (d) Dunlop-Brière, A. F.; Baird, M. C.; Budzelaar, P. H. M. *Organometallics* **2015**, 34, 2356.
- (5) A number of computational papers consider the interplay between  $\alpha$ - and  $\beta$ -agostic species. See: (a) Nifant'ev, I. E.; Ustynyuk, L. Y.; Laikov, D. N. *Organometallics* **2001**, 20, 5375. (b) Graf, M.; Angermund, K.; Fink, G.; Thiel, W.; Jensen, V. R. *J. Organomet. Chem.* **2006**, 691, 4367. (c) Karttunen, V. A.; Linnolahti, M.; Pakkanen, T. A.; Severn, J. R.; Kokko, E.; Maaranen, J.; Pitkänen, P. *Organometallics* **2008**, 27, 3390.
- (6) (a) Hayakawa, K.; Kawase, K.; Yamakita, H.; Inagaki, S. *J. Polym. Sci., Part B: Polym. Lett.* **1967**, 5, 1077. (b) Hayakawa, K.; Kawase, K.; Yamakita, H.; Yumoto, T. *J. Polym. Sci., Polym. Chem. Ed.* **1981**, 19, 3145.
- (7) (a) Ahlrichs, R.; Armbruster, M. K.; Bachorz, R. A.; Bär, M.; Baron, H.-P.; Bauernschmitt, R.; Bischoff, F. A.; Böcker, S.; Crawford, N.; Deglmann, P.; Della Sala, F.; Diedenhofen, M.; Ehrig, M.; Eichkorn, K.; Elliott, S.; Friese, D.; Furche, F.; Glöss, A.; Haase, F.; Häser, M.; Hättig, C.; Hellweg, A.; Höfener, S.; Horn, H.; Huber, C.; Huniar, U.; Kattannek, M.; Klopper, W.; Köhn, A.; Kölmel, C.; Kollwitz, M.; May, K.; Nava, P.; Ochsenfeld, C.; Öhm, H.; Pabst, M.; Patzelt, H.; Rappoport, D.; Rubner, O.; Schäfer, A.; Schneider, U.; Sierka, M.; Tew, D. P.; Treutler, O.; Unterreiner, B.; von Arnim, M.; Weigend, F.; Weis, P.; Weiss, H.; Winter, N. *Turbomole*, version 5; Theoretical Chemistry Group, University of Karlsruhe: Karlsruhe, Germany, 2002. (b) Treutler, O.; Ahlrichs, R. *J. Chem. Phys.* **1995**, 102, 346. (c) Schäfer, A.; Huber, C.; Ahlrichs, R. *J. Chem. Phys.* **1994**, 100, 5829. (d) Tao, J. M.; Perdew, J. P.; Staroverov, V. N.; Scuseria, G. E. *Phys. Rev. Lett.* **2003**, 91, article 146401. (e) PQS, version 2.4; Parallel Quantum Solutions: Fayetteville, AR, 2001 (the Baker optimizer is available separately from PQS upon request). (f) Baker, J. *J. Comput. Chem.* **1986**, 7, 385.
- (8) (a) Frisch, M. J.; Trucks, G. W.; Schlegel, H. B.; Scuseria, G. E.; Robb, M. A.; Cheeseman, J. R.; Montgomery, J. A., Jr.; Vreven, T.; Kudin, K. N.; Burant, J. C.; Millam, J. M.; Iyengar, S. S.; Tomasi, J.; Barone, V.; Mennucci, B.; Cossi, M.; Scalmani, G.; Rega, N.; Petersson, G. A.; Nakatsuji, H.; Hada, M.; Ehara, M.; Toyota, K.; Fukuda, R.; Hasegawa, J.; Ishida, M.; Nakajima, T.; Honda, Y.; Kitao, O.; Nakai, H.; Klene, M.; Li, X.; Knox, J. E.; Hratchian, H. P.; Cross, J. B.; Bakken, V.; Adamo, C.; Jaramillo, J.; Gomperts, R.; Stratmann, R. E.; Yazyev, O.; Austin, A. J.; Cammi, R.; Pomelli, C.; Ochterski, J. W.; Ayala, P. Y.; Morokuma, K.; Voth, G. A.; Salvador, P.; Dannenberg, J. J.; Zakrzewski, V. G.; Dapprich, S.; Daniels, A. D.; Strain, M. C.; Farkas, O.; Malick, D. K.; Rabuck, A. D.; Raghavachari, K.; Foresman, J. B.; Ortiz, J. V.; Cui, Q.; Baboul, A. G.; Clifford, S.; Cioslowski, J.; Stefanov, B. B.; Liu, G.; Liashenko, A.; Piskorz, P.; Komaromi, I.; Martin, R. L.; Fox, D. J.; Keith, T.; Al-Laham, M. A.; Peng, C. Y.; Nanayakkara, A.; Challacombe, M.; Gill, P. M. W.; Johnson, B.; Chen, W.; Wong, M. W.; Gonzalez, C.; Pople, J. A. *Gaussian 03*, revision C.02; Gaussian, Inc.: Wallingford, CT, 2004. (b) Zhao, Y.; Truhlar, D. G. *Theor. Chem. Acc.* **2008**, 120, 215. (c) Ehm, C.; Budzelaar, P. H. M.; Busico, V. *J. Organomet. Chem.* **2015**, 775, 39. (d) Dunning, T. H. *J. Chem. Phys.* **1989**, 90, 1007. (e) Kendall, R. A.; Dunning, T. H.; Harrison, R. J. *J. Chem. Phys.* **1992**, 96, 6796. (f) Woon, D. E.; Dunning, T. H. *J. Chem. Phys.* **1993**, 98, 1358. (g) Balabanov, N. B.; Peterson, K. A. *J. Chem. Phys.* **2005**, 123, 064107. (h) Feller, D. *J. Comput. Chem.* **1996**, 17, 1571. (i) Schuchardt, K. L.; Didier, B. T.; Elsethagen, T.; Sun, L. S.; Gurumoorthis, V.; Chase, J.; Li, J.; Windus, T. L. *J. Chem. Inf. Model.* **2007**, 47, 1045.
- (9) (a) Tobisch, S.; Ziegler, T. *J. Am. Chem. Soc.* **2004**, 126, 9059. (b) Raucoles, R.; De Bruin, T.; Raybaud, P.; Adamo, C. *Organometallics* **2009**, 28, 5358. (c) Ditchfield, R. *Mol. Phys.* **1974**, 27, 789. (d) Wolinski, K.; Hinton, J. F.; Pulay, P. *J. Am. Chem. Soc.* **1990**, 112, 8251.
- (10) (a) Kutzelnigg, W.; Fleischer, U.; Schindler, M. The IGLO-Method: Ab Initio Calculation and Interpretation of NMR Chemical Shifts and Magnetic Susceptibilities. In *NMR Basic Principles and Progress*; Diehl, P.; Flück, E.; Günther, H.; Kosfeld, R.; Seelig, J., Eds.; Springer-Verlag: Heidelberg, Germany, 1990; Vol. 23. (b) Budzelaar, P. H. M. *gNMR*, VS.1, NMR simulation package; University of



Manitoba. <http://home.cc.umanitoba.ca/~budzelaa/gNMR/gNMR.html>. For the ABX spin system of **IV**, analysis of the multiplet at  $\delta \sim 4.3$  at 225 K involved a full least-squares fit of the data and was carried out with the approximations that  $J_{\alpha-\gamma} = 0$  Hz and that the line width chosen for the simulation to match the experimental spectrum) was 1.50 Hz. In addition, the three  $\gamma$ -H were set to their averaged chemical shift value. (c) For a very useful discussion of spectral patterns of AA'XX' spin systems, see Reich, H. J. 2015, <http://www.chem.wisc.edu/areas/reich/nmr/05-hmr-14-a2b2.htm#05-hmr-14-a2b2-geminal>.

(11) (a) A reviewer notes that our lowest temperature spectrum was obtained below the freezing point of the solvent (176 K) and suggests that overlooked freezing of the solution may have caused the broadening. We think not since other resonances remained relatively narrow and, as we have noted previously,<sup>11b</sup> supercooling of NMR solutions in the confines of a 5 mm NMR tube has precedent.

(b) Vatamanu, M.; Stojcevic, G.; Baird, M. C. *J. Am. Chem. Soc.* **2008**, 130, 454 ref 9..

(12) (a) Creary, X.; Kochly, E. D. *J. Org. Chem.* **2009**, 74, 9044.

(b) Creary, X. *J. Am. Chem. Soc.* **2013**, 135, 6570. (c) Creary, X.; Heffron, A.; Going, G.; Prado, M. *J. Org. Chem.* **2015**, 80, 1781.

(13) Jung, M. E.; Piizzi, G. *Chem. Rev.* **2005**, 105, 1735.